Implications of within-scan patient head motion on B_1^+-homogeneity and Specific Absorption Rate at 7T

Emre Kopanoglu[1], Alix Plumley[1], Cem M. Deniz[2], Arcan M. Erturk[3,4], Richard G. Wise[1]

[1] Cardiff University Brain Research Imaging Centre (CUBRIC), School of Psychology, Cardiff University, Cardiff, UK
[2] Department of Radiology, New York University School of Medicine, New York, NY 10016 USA
[3] Medtronic, Restorative Therapies Group, Minneapolis, Minnesota, USA
[4] University of Minnesota, Center for Magnetic Resonance Research, Minneapolis, Minnesota, USA

Synopsis
Parallel-transmit pulses are commonly used to improve B_1^+-homogeneity at higher field strengths, while local-SAR constraints are applied to ensure safety. However, patient motion may become unavoidable with longer scans or less cooperative patients, and motion may affect B_1^+-homogeneity and local-SAR. We investigated the effect of all 6 degrees-of-freedom of head motion on B_1^+-homogeneity and local-SAR for parallel-transmit multi-spoke pulses using simulations. We observed more than a 2-fold increase in local-SAR due to motion for some pulses. We also investigated the changes in B_1^+-homogeneity of spokes pulses using in-vivo B_1^+-maps and showed regional variations between 12%-22% in the excitation profile.

Introduction
The use of multi-channel parallel-transmit (pTx) arrays has been commonly investigated to improve B_1^+-homogeneity at higher field strengths (7T). However, the possibility of creating local-SAR/local-temperature hotspots due to constructive interference of the electric field has raised questions on safety. Thus, local-SAR/local-temperature has been used as a safety constraint in pulse design, and several safety margins have been applied in practice to account for modelling imperfections[1-10]. However, the effect of patient motion on B_1^+-homogeneity and safety remains as an important question that has received little attention. Patient motion might become unavoidable especially with longer scans or less cooperative patients, such as in pediatric imaging[11-14], or for patients with Parkinson's[15] or dementia[16].

Earlier studies have investigated the effect of body position on B_1^+-homogeneity and local-SAR[17-20]. However, these studies have been limited to a subset of motion types and have focussed on the initial positioning of the patient rather than motion during the scan. In this study, we investigate, using simulation, the effect of all 6 degrees-of-freedom head motion during scan on B_1^+-homogeneity and local-SAR for multi-spoke pulses. Moreover, we show the effect of head motion on excitation profiles at 7T using in-vivo B_1^+-maps of an 8-channel pTx coil.

Methods
Simulations were conducted using Sim4Life (ZMT, Zurich, Switzerland) for an 8-channel loop array and the body model Ella (IT'IS, Zurich, Switzerland). Patient motion was modelled by keeping the body model stationary and moving the RF array. This approach **i)** prevents changes in electromagnetic properties of the model due to voxelization effects as it keeps the tissues in the body model intact, **ii)** isolates the B_1^+-related effects as no image-registration is required. The array was **i)** displaced along or rotated around

the three main axis, and **ii)** displaced along two-dimensions on coronal and axial planes for a total of 105 positions. Displacements and rotations of 1/2/5/10/15/20 mm or degrees were simulated, unless the prescribed motion would overlap the coil and the body model. Adaptive voxelization was used with maximum voxel size of 2mm for the model and <40% of conductor width for the array. Coil elements were checked for connectivity and voxelization prior to simulation.

For six different axial slices (each separated by 18mm), 1-, 2-, 3-spokes RF excitation pulses were designed to optimize for in-slice B_1^+-homogeneity[21]. Normalized root-mean-squared error (nRMSE) was calculated on the complex excitation profiles since phase changes also contribute to error due to motion in practice. 1-gram averaged maximum local-SAR was calculated for each relative position of the model and normalized by the maximum local-SAR for the case without motion.

In vivo experiments were conducted on a 7T scanner (Siemens Healthcare, Erlangen, Germany) with an 8-/32-channel pTx/Rx coil (Nova Medical, MA, USA). The participant moved his head between scans while B_1^+-maps and GRE images were acquired. Images were registered using masks created from the GRE images and head motion was estimated to be Right/Anterior/Yaw: -2.6mm/7.5mm/0degree (position2), 5.6mm/15.5mm/1.6degree (position3), 5.4mm/0.4mm/0.9degree (position4). 1-/2-/3-spoke pulses were designed using the B_1^+-maps acquired in the first position. Using the in-vivo B_1^+-maps acquired at different positions, the excitation profiles of the designed pulses were simulated. The difference between the excitation profiles due to participant motion were analysed.

Results

Figure 1 shows the variation of nRMSE for a 3-spoke pulse designed for imaging the temporal lobe. The excitation profile was more sensitive to in-slice motion (right-left, anterior-posterior and yaw). Figure 2 demonstrates the change in the profile as the body model rotates in yaw. Figure 3 shows that, while the inner-slices are more sensitive to in-(axial-)slice motion, the outer slices (cerebellum/crown) are more susceptible to superior-inferior, roll and pitch motion.

Figure 4 shows the change in the maximum local-SAR observed for all 18 pulses. In 3% of the cases, the maximum local-SAR increased by more than 50% compared to the respective maximum local-SAR at the centre position and increased by more than 2-fold in ten cases. For one slice/pulse combination, local-SAR increased with a slope of 6.5%-per-mm of lateral motion.

Figure 5 shows the changes in the excitation profiles simulated using in-vivo B_1^+-maps. The head motion caused 12%-22% change in the excitation profiles.

Discussion

We have demonstrated that the B_1^+-homogeneity created via multi-spoke pTx pulses is highly susceptible to within-scan patient motion. This is especially important for patient populations that may not stay still for extended durations[11-16]. More importantly, the results showed that maximum local-SAR is highly sensitive to motion for some slice/pulse combinations (rather than just motion extent) and rapidly increases with the amount of motion. Finally, the range of increase in maximum local-SAR due to motion is similar to previous literature, although we observed the maximum increase for lateral displacement which was excluded inRefs[17-20].

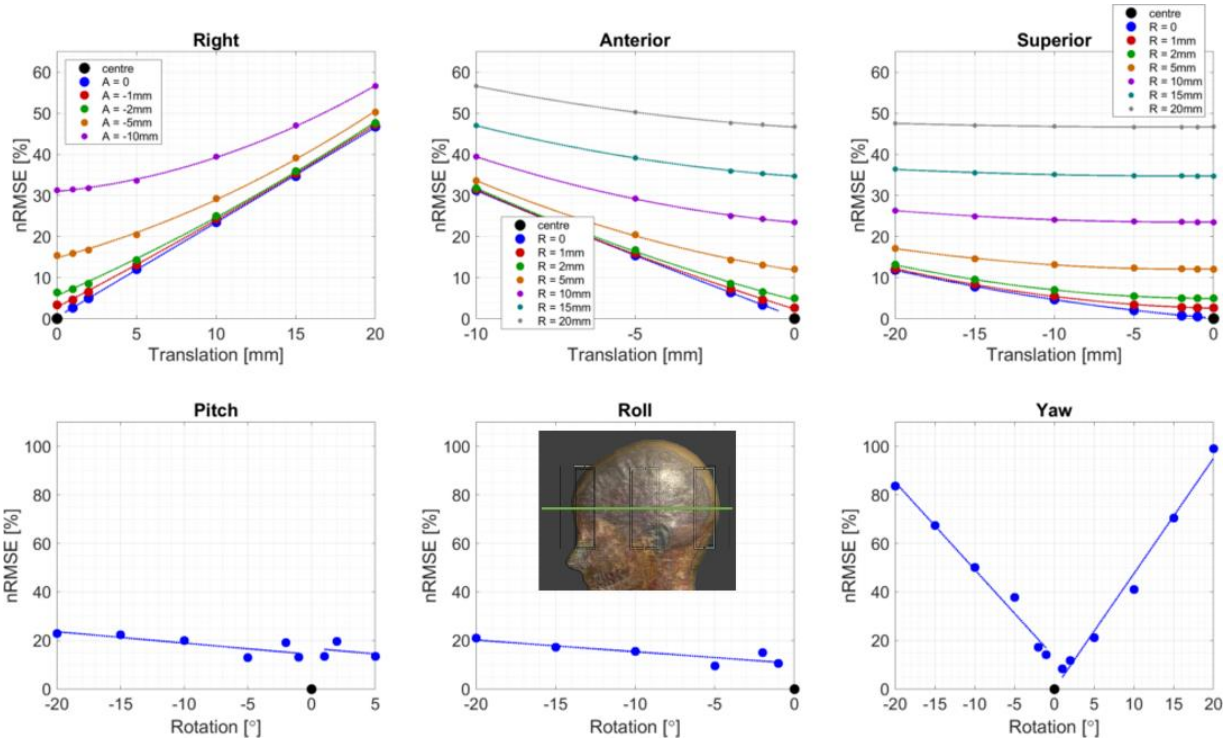

Figure 1: The nRMSE in the excitation profile compared to the initial (centre, denoted by the black dot) position is given for all six degrees-of-freedom of motion: displacement along right-left, anterior-posterior, superior-inferior; and rotation in pitch, roll and yaw. Panels in the top row also show off-axis motion on the axial (left, centre) and coronal planes (right). Inset shows the slice the pulse was designed for. In this slice, B_1^+-homogeneity was less sensitive to motion in superior-inferior, pitch and roll; the nRMSE increased rapidly with radial displacement (2.4%-per-mm, graph not shown) and rotation (4.6%-per-degree) on the axial plane.

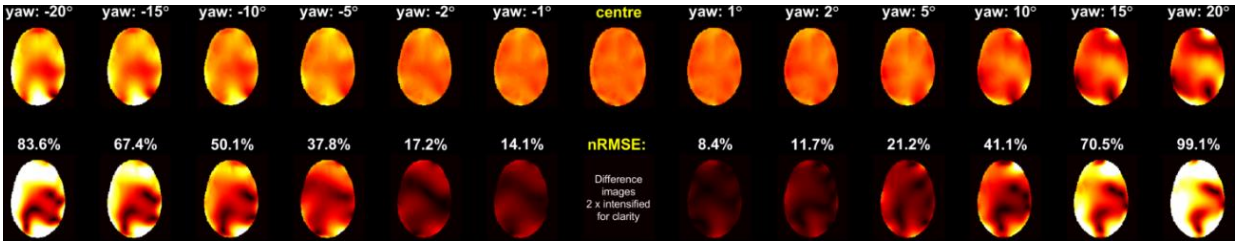

Figure 2: The variation in the excitation profile of a 3-spoke pulse (same slice as Figure 1) is demonstrated for rotational motion around the z-axis (yaw). As expected, the intensity of the difference images increases with the amount of rotation. The difference between channel weights becomes apparent as the change due to motion is non-trivial and highly spatially-varying. Contrarily, for quadrature mode with a 1-spoke pulse (equal-amplitudes, progressive phase-increments), the error is dominated by a global phase change due to rotation while the effects of coil loading are less pronounced, and the error images resemble scaled versions of the magnitude excitation profile (data not shown).

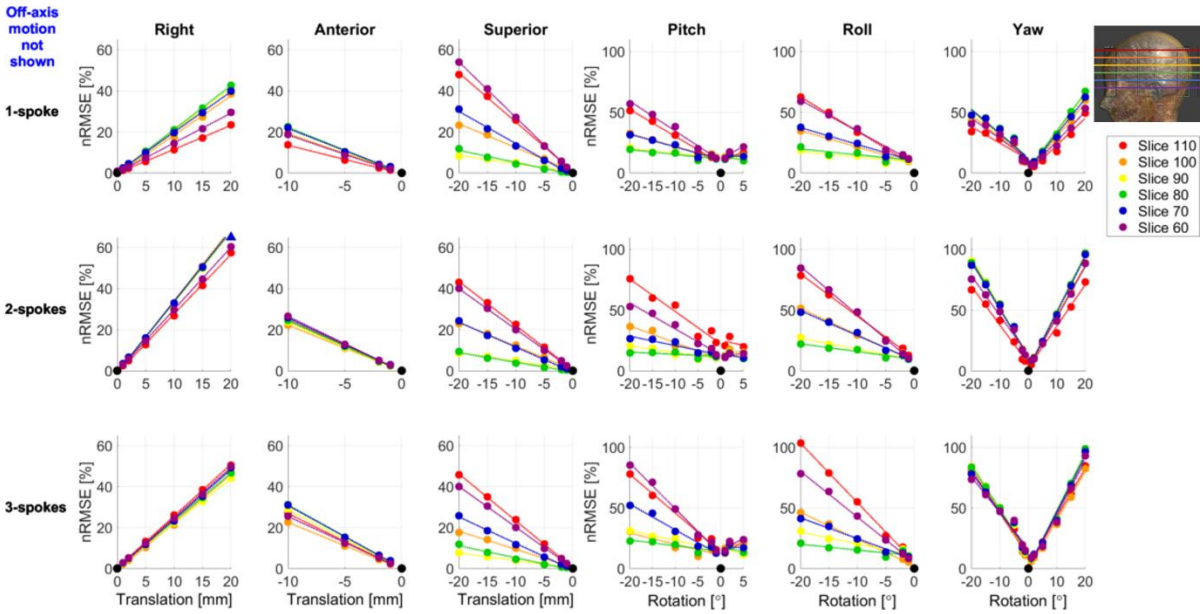

Figure 3: The nRMSE in the excitation profile is calculated for six different 3-spoke pulses designed to minimize the in-slice B_1^+-inhomogeneity in six different slices (slice locations shown on the right). Off-axis cases on the axial and coronal planes were omitted for clarity. While the slices in the centre are more susceptible to motion in the axial plane (right-left, anterior-posterior, yaw), the outer slices are more susceptible to motion in superior-inferior, pitch and roll.

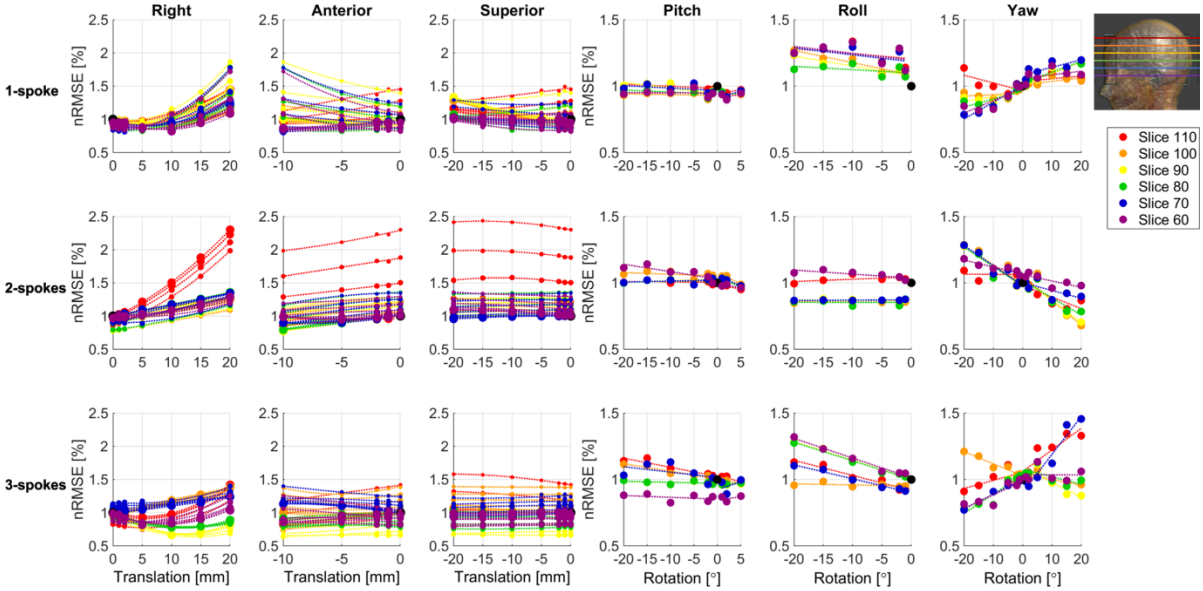

Figure 4: The change in the maximum local-SAR due to motion is shown for 1-spoke, 2-spoke and 3-spoke pulses for all slices (slice locations shown on the right). The maximum local-SAR for any slice/pulse was normalized by the maximum local-SAR of the same pulse without motion. The maximum local-SAR increased by more than 2-fold in 10 cases, and more than 50% in a total of 57 (3%) cases (note that datapoints for axial and coronal motion are displayed on multiple panels). The extreme increases in maximum local-SAR do not depend only on the amount of displacement/rotation, which prevents determining safety margins for different motion types.

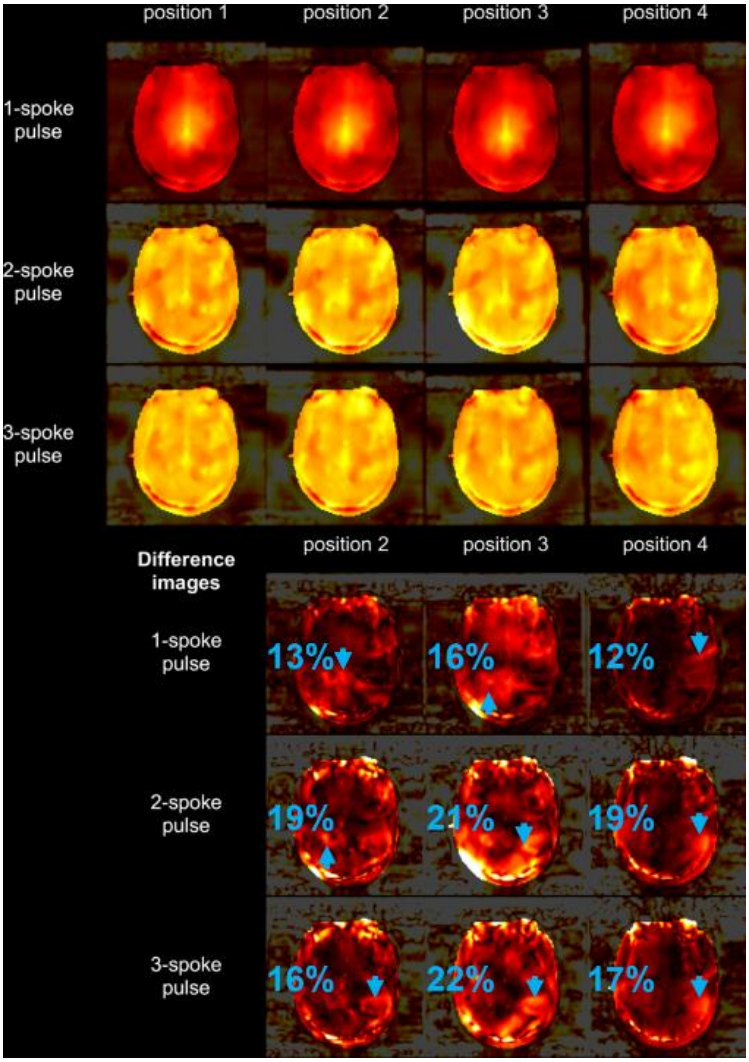

Figure 5: Excitation profiles were simulated for 1-spoke, 2-spoke, 3-spoke pulses using in-vivo B_1^+-maps. Pulses were designed to generate 90^o flip angle around the centre of the field of view for position 1. All B_1^+-maps were registered to the first position before calculating the profiles. **Rows 1-3:** Excitation profiles simulated using in-vivo B_1^+-maps. **Rows 4-6:** Complex difference images calculated with respect to the respective excitation profiles at position 1. Arrows indicate the regions where reported values were calculated (isolated variations confined to a few voxels were not used in analysis). Variations between 12% and 22% were observed in the simulated excitation profiles.

REFERENCES

1. Cloos MA, Luong M, Ferrand G, Amadon A, Le Bihan D, Boulant N. Local SAR reduction in parallel excitation based on channel-dependent Tikhonov parameters. Journal of Magnetic Resonance Imaging 2010;32(5):1209-1216.
2. Lee J, Gebhardt M, Wald LL, Adalsteinsson E. Local SAR in parallel transmission pulse design. Magn Reson Med 2012;67(6):1566-1578.
3. Wu X, Schmitter S, Auerbach EJ, Moeller S, Ugurbil K, Van de Moortele PF. Simultaneous multislice multiband parallel radiofrequency excitation with independent slice-specific transmit B1 homogenization. Magn Reson Med 2013;70(3):630-638.

4. Guerin B, Setsompop K, Ye H, Poser BA, Stenger AV, Wald LL. Design of parallel transmission pulses for simultaneous multislice with explicit control for peak power and local specific absorption rate. Magn Reson Med 2015;73(5):1946-1953.
5. Guerin B, Gebhardt M, Serano P, Adalsteinsson E, Hamm M, Pfeuffer J, Nistler J, Wald LL. Comparison of simulated parallel transmit body arrays at 3 T using excitation uniformity, global SAR, local SAR, and power efficiency metrics. Magn Reson Med 2015;73(3):1137-1150.
6. Deniz CM, Carluccio G, Sodickson DK, Collins CM. Non-Iterative Parallel Transmission RF Pulse Design with Strict Temperature Constraints. 2015; Toronto, Canada. p 549.
7. Wu X, Schmitter S, Auerbach EJ, Ugurbil K, Van de Moortele PF. A generalized slab-wise framework for parallel transmit multiband RF pulse design. Magn Reson Med 2016;75(4):1444-1456.
8. Vinding MS, Guerin B, Vosegaard T, Nielsen NC. Local SAR, global SAR, and power-constrained large-flip-angle pulses with optimal control and virtual observation points. Magn Reson Med 2017;77(1):374-384.
9. Deniz CM, Carluccio G, Collins C. Parallel transmission RF pulse design with strict temperature constraints. NMR Biomed 2017;30(5):e3694-n/a.
10. Gras V, Boland M, Vignaud A, Ferrand G, Amadon A, Mauconduit F, Le Bihan D, Stöcker T, Boulant N. Homogeneous non-selective and slice-selective parallel-transmit excitations at 7 Tesla with universal pulses: A validation study on two commercial RF coils. PloS one 2017;12(8):e0183562-e0183562.
11. Malviya S, Voepel-Lewis T, Eldevik OP, Rockwell DT, Wong JH, Tait AR. Sedation and general anaesthesia in children undergoing MRI and CT: adverse events and outcomes. Br J Anaesth 2000;84(6):743-748.
12. Havidich JE, Beach M, Dierdorf SF, Onega T, Suresh G, Cravero JP. Preterm Versus Term Children: Analysis of Sedation/Anesthesia Adverse Events and Longitudinal Risk. Pediatrics 2016;137(3):e20150463.
13. Mallory MD, Travers C, McCracken CE, Hertzog J, Cravero JP. Upper Respiratory Infections and Airway Adverse Events in Pediatric Procedural Sedation. Pediatrics 2017;140(1).
14. Boriosi JP, Eickhoff JC, Klein KB, Hollman GA. A retrospective comparison of propofol alone to propofol in combination with dexmedetomidine for pediatric 3T MRI sedation. Paediatr Anaesth 2017;27(1):52-59.
15. Schwarz ST, Afzal M, Morgan PS, Bajaj N, Gowland PA, Auer DP. The 'swallow tail' appearance of the healthy nigrosome - a new accurate test of Parkinson's disease: a case-control and retrospective cross-sectional MRI study at 3T. PLoS One 2014;9(4):e93814.
16. Prasher V, Cumella S, Natarajan K, Rolfe E, Shah S, Haque MS. Magnetic resonance imaging, Down's syndrome and Alzheimer's disease: research and clinical implications. J Intellect Disabil Res 2003;47(Pt 2):90-100.
17. Shao Y, Zeng P, Wang S. Statistical simulation of SAR variability with geometric and tissue property changes by using the unscented transform. Magn Reson Med 2015;73(6):2357-2362.
18. Le Garrec M, Gras V, Hang MF, Ferrand G, Luong M, Boulant N. Probabilistic analysis of the specific absorption rate intersubject variability safety factor in parallel transmission MRI. Magn Reson Med 2017;78(3):1217-1223.
19. Murbach M, Zastrow E, Kuster N. Virtual Population Based Correlations between B1+, Whole-Body and Local SAR. 2018; Paris, France. p 4391.
20. Kozlov M, Turner R. Effects of tuning condition, head size and position on the SAR of MRI dual-row transmit arrays. 2013 6-10 Oct. 2013. p 708-711.
21. Kopanoglu E. Near real-time parallel-transmit pulse design. 2018; Paris, France. p 3392.